

Synthesis of a merlinoite-type zeolite with an enhanced Si/Al ratio *via* pore filling with tetraethylammonium cations

Philip A. Barrett, Susana Valencia and Miguel A. Cambor*

Instituto de Tecnología Química, CSIC-UPV, Universidad Politécnica de Valencia, Avda. los Naranjos s/n, 46071 Valencia, Spain

Received 20th May 1998, Accepted 24th June 1998

A merlinoite type zeolite with an enhanced Si/Al ratio (around 3.8) compared to known isostructural materials has been synthesised hydrothermally from a gel with Si/Al = 5 in the presence of tetraethylammonium and K^+ cations. The zeolite has been characterised by a number of techniques and in its calcined form the structure was refined from synchrotron powder X-ray diffraction data [$a = 14.1291(10)$, $b = 14.1308(10)$, $c = 9.9274(5)$ Å, *Immm*]. The different techniques reveal the enhanced Si/Al ratio of the zeolite. Tetraethylammonium is occluded within the tridimensional small pore channels, forcing the K^+ and hence the Al content to diminish by 30–50% compared to conventional merlinoite-type zeolites. The thermal stability of the material is greatly improved, although if K^+ cations in the zeolite are exchanged by NH_4^+ the stability decreases as a function of the degree of exchange, suggesting a low stability for the acidic form of merlinoite.

Introduction

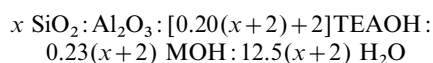
Merlinoite is a small pore zeolite characterised by a low Si/Al ratio and its tridimensional interconnected 8 member ring (8MR) channel system. While it is found in nature as a rare mineral it has also been synthesised in the laboratory and given different names including K-M and Linde W. All the natural and synthetic merlinoite-type zeolites reported so far have a narrow window of Si/Al ratios in the range 1.5–2.4. On the other hand, even when synthesised in the presence of both inorganic and organic cations only inorganic cations were found within the pores.¹

It is well established since the original work of Barrer and Denny² that the use of organic cations in the synthesis of zeolites may result in products with an enhanced Si/Al ratio. In general the volume occupied by one occluded organic cation within the zeolite framework is much larger than that occupied by an inorganic cation. This leads to a reduction in the counter cation concentration within the zeolite pores and hence to a lower $AlO_{4/2}^-$ concentration in the framework. From a catalytic standpoint this is important, since an increase in the Si/Al ratio of zeolites generally enhances their thermal stability whilst although the concentration of Brønsted acid sites when the counter cations are H^+ is decreased their acid strength is increased. Here we present the synthesis and characterisation of a merlinoite-type zeolite using potassium as well as tetraethylammonium cations in the nutrient gel. Incorporation of the large organic cations allows the crystallisation of a zeolite with a significantly higher Si/Al ratio and an enhanced thermal stability.

Experimental

Synthesis

Amorphous silica (Aerosil 200, Degussa) was added to a 35% aqueous solution of tetraethylammonium hydroxide ($TEA^+ OH^-$, Aldrich, $Na < 2$ ppm, $K < 60$ ppm) and the resulting mixture was stirred mechanically. To this mixture, a solution made by dissolving metal Al in TEAOH and KOH or NaOH was added and the mixture was further homogenised mechanically. The final gel composition can be expressed as



The SiO_2/Al_2O_3 ratio (x) was varied between 6 and 14 (Table 1) and the $M/(Si+Al)$ was kept constant at 0.23 with $M = Na^+$ or K^+ . The concentration of TEAOH was varied to keep the alkalinity constant at a $(OH^- - Al)/(Si+Al)$ ratio of 0.43. The $H_2O/(Si+Al)$ ratio was fixed at 12.5.

The mixture was crystallised in Teflon lined 60 ml autoclaves heated at 140 °C under slow rotation (60 rpm). After cooling down, the autoclaves the contents were centrifuged, and the resultant solids washed with distilled water until pH < 9 and dried at 100 °C.

Characterisation

Phase purity and crystallinity were determined by conventional powder X-ray diffraction (XRD) using a Philips X'Pert diffractometer (Cu-K α radiation, graphite monochromator) provided with a variable divergence slit and working in the fixed irradiated area mode. *In situ* XRD measurements at high temperature were recorded on the same apparatus using an Anton Parr HTK 16 camera provided with a 1 mm thick Pt filament. Thermogravimetric analyses were performed on a Netzsch STA 409 EP thermal analyser in the range 293–1023 K with ca. 0.0200 g of sample, a heating rate of 10 K min⁻¹ and an air flow of 61 h⁻¹. C, H and N contents were determined with a Carlo Erba 1106 elemental organic analyser. Al and K contents were determined with a Varian SpectraAA-10Plus. MAS NMR spectra of the solids were recorded on a Varian VXR 400SWB spectrometer. The ²⁹Si MAS NMR spectra were recorded with a spinning rate of 5.5 kHz at a ²⁹Si frequency of 79.459 MHz with a 55.4° pulse length of 4.0 s and a recycle delay of 60 s. The ¹³C MAS NMR spectrum was acquired with a spinning rate of 5 kHz at a ¹³C frequency of 100.577 MHz with a 90° pulse length of 7.5 μ s and a recycle

Table 1 Summary of the synthesis results

SiO_2/Al_2O_3	M^+	Time/days	Product
6	K^+	35	amorphous
10	K^+	14	MER ^a
10	Na^+	7	beta + ANA
10	Na^+	34	ANA + beta
14	K^+	7	MER + beta
14	K^+	16	beta + MER

^aSample used for structure refinement. Contains $\approx 1\%$ zeolite beta.

Table 2 Data collection and crystallographic parameters for merlinoite

Wavelength/Å	1.200511
2θ range/°	10–80
Step size/°	0.01
Count time/s	2
Number of data points	6353
Number of reflections	647
Number of profile parameters	10
Number of structural parameters	38
Unit cell	
<i>a</i> /Å	14.1291(10)
<i>b</i> /Å	14.1308(10)
<i>c</i> /Å	9.9274(5)
Cell volume/Å ³	1982.06(22)
Space group	<i>Immm</i>
Residuals	
<i>R</i> _{exp}	5.58
<i>R</i> _p	6.82
<i>R</i> _{wp}	8.69
<i>R</i> _b	8.29
χ ²	2.45

delay of 15 s. Both ²⁹Si and ¹³C chemical shifts are reported relative to TMS. The ²⁷Al MAS NMR spectra were recorded with a spinning rate of 7 kHz at a ²⁷Al frequency of 104.218 MHz with a 10° pulse length of 0.5 μs and a recycle delay of 0.5 s, and the chemical shift is reported relative to Al(H₂O)₆³⁺. The IR spectrum in the region of framework vibrations (300–1900 cm⁻¹) was recorded in a Nicolet 710 FTIR spectrometer using the KBr pellet technique.

XRD data collection and refinement

Flat plate high resolution powder diffraction data were recorded on a freshly calcined sample of high silica merlinoite (see Table 1), on station 2.3 of the Daresbury SRS using the parameters summarised in Table 2. The data were normalised before Rietveld refinement³ was undertaken in the program GSAS.⁴ A model for the framework atomic positions was taken from the structure reported by Bieniok *et al.*⁵ for a merlinoite of composition K_{10.3}[Si_{21.7}Al_{10.3}O₆₄]. A manually interpolated background and a pseudo-Voigt⁶ function to describe the peak shape were used. After initial refinement of the scale factor, cell parameters, zero point and the peak shape a small quantity of a zeolite beta impurity phase was observed and excluded from the refinement. A difference Fourier map was calculated at this point which revealed two strong peaks which were tested as potassium sites and a number of weaker peaks assumed to be water molecules. The position of the two potassium sites were found to coincide with two of the four sites found from the work of Bieniok *et al.*⁵ The two K positions were included into the model and refinement of their occupancy together with the atomic positions and temperature factors led to agreement factors⁴ of *R*_{wp}=18.5, *R*_p=12.3. A second difference Fourier map was calculated at this point revealing five strong peaks which were included into the model as water sites. Refinement of the occupancy for these sites showed them to be stable in the refinement and that the quantity of extra framework water was close to that expected from chemical analysis. However for OW(4) the maximum permitted occupancy was fixed to be 0.5 to eliminate unrealistic symmetry related contacts. In the final cycles of refinement all atomic positions and temperature factors (apart from the temperature factors for the extra framework water sites which were constrained so as to be equal) were refined with the final model converging to *R*_{wp}=8.69, *R*_p=6.82 and *R*_b=8.29 (*R*_{exp}=5.58).

Results and discussion

The synthesis results presented in Table 1 show that K⁺ exerts a significant structure-directing effect when the conditions reported above are used. Whilst synthesis in the presence of

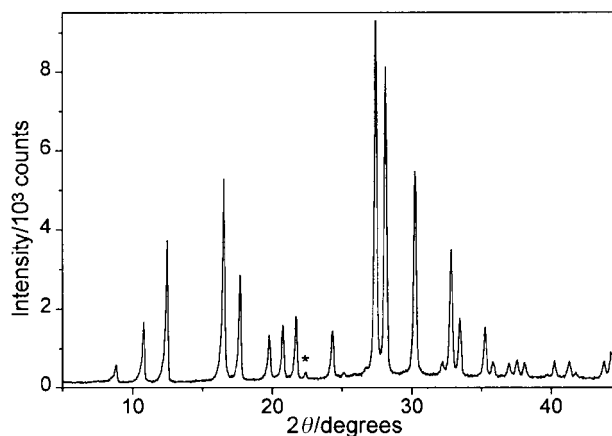


Fig. 1 Powder XRD pattern of as-made merlinoite. A small zeolite beta impurity (≈1%) is marked with an asterisk.

Na⁺ yields a mixture of zeolite beta and analcime (ANA), the presence of K⁺ in a gel with Si/Al=5 leads to a merlinoite-type zeolite having the characteristic XRD pattern shown in Fig. 1. We note however that a very weak peak at 2θ≈22.4°, not belonging to merlinoite, was detected. In the synchrotron XRD data five additional very small and broad peaks were also detected enabling us to identify this impurity phase as zeolite beta. From the area of the peak at 22.4° the relative proportion of the beta impurity was estimated as *ca.* 1%.

Structure-direction by inorganic cations⁷ appears frequently in the synthesis of zeolites with low Si/Al ratios, although it is less common for syntheses in the presence of organic additives whose structure-directing ability usually surpasses that of the alkali metal cations. It is notable that for very similar synthesis conditions but with lower Al content the products are zeolite beta irrespective of the type of inorganic cation present (Na⁺, K⁺ or any mixture of Na⁺ and K⁺).⁹ From Table 1, when the Si/Al ratio of the initial mixture is decreased to three or increased to seven using K⁺ cations the synthesis product is amorphous or a mixture of merlinoite and zeolite beta, respectively. Thus, in the presence of tetraethylammonium a relatively narrow window of compositions exists for the synthesis of merlinoite.

The chemical composition of the merlinoite-type zeolite produced in this work is presented in Table 3. For the unit cell composition, [C₈H₂₀N]_{0.8}H_{0.7}K_{5.2}[Al_{6.7}Si_{25.3}O₆₄].12H₂O, we need to introduce a minor amount of H⁺ to account for a small misbalance between the counter cations (K⁺+TEA⁺) and Al. The Si/Al ratio of our zeolite is found to be 3.8 and is significantly higher than that of previously reported merlinoite-type materials. It is noteworthy that in the absence of tetraethylammonium K-M zeolite (a merlinoite-type material) could be synthesised from gels with an initial Si/Al ratio in the range 0.5–5, while the product of the synthesis had a fairly constant Si/Al ratio (1.5–1.7).⁷ To the best of our knowledge, reported Si/Al ratios for merlinoite-type zeolites are always in the range 1.5–2.4. There is a wider variability for the natural mineral (Si/Al=1.6–2.4),¹⁰ than for the synthetic analogues (Si/Al=1.5–1.75,⁷ 1.8–1.9,¹¹ 1.75,¹² 1.7,¹³ 2.1⁵). Thus, merlinoite appears to be one of the so-called low silica zeolites for which, typically, the Si/Al ratio is not only low

Table 3 Chemical composition of merlinoite

	K	Al	C	N	H	H ₂ O ^a	TEA ⁺ ^a
Wt.%	8.2	7.3	3.00	0.48	1.4	8.88	4.33
Per u.c.	5.2	6.7	6.2	0.8	—	12.1	0.8

^aFrom TGA (H₂O < 270 °C; TEA⁺ > 350 °C).

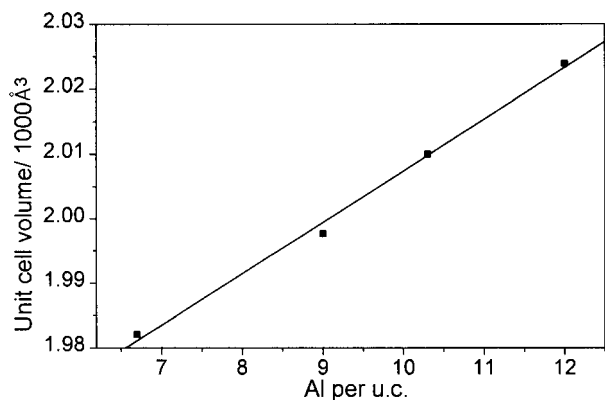


Fig. 2 Variation of the orthorhombic unit cell volume of synthetic and natural merlinoites as a function of their Al content.

but also constrained within a fairly small range of values. Increasing the Si/Al ratios in such materials by direct synthesis is generally difficult and may require the use of organic additives. Adopting this strategy under the conditions described in this work we have demonstrated that it is possible to reduce the Al content of merlinoite by 35–50% compared to other reported synthetic materials. When the unit cell volume of the merlinoite presented in this work is compared with those of other synthetic or natural orthorhombic merlinoites in which K^+ is the main counter cation a linear correlation between unit cell volume and Al content is obtained (Fig. 2). From this correlation an expansion coefficient of 0.155 for the isomorphous substitution of Si by Al in merlinoite is obtained.† The decreased unit cell volume of the merlinoite presented in this work confirms its lower Al content.

As shown in Table 3, there is a significant amount of organic matter within the final zeolite. The C/N ratio of our as-made zeolite is close to, although slightly smaller than the theoretical value for TEA,⁸ suggesting that most of the occluded organic remains intact as TEA^+ cations inside the zeolite pores. ¹³C MAS NMR of as-made merlinoite shows two bands at δ 51.5 and 8.1 assigned to the methylene and methyl groups, respectively, of TEA^+ . Interestingly, in previous reports concerning the synthesis of merlinoite-type materials from gels containing mixtures of K^+ and tetramethylammonium (TMA^+) or K^+ , Na^+ and TMA^+ , no organics were found in the zeolite.¹ The conclusion drawn from these experiments was that this zeolite structure could not accommodate the large TMA^+ cations. Obviously, this is not the case since we have found the even larger TEA^+ in our final product. There are around 0.8 TEA^+ cations per unit cell of 32 T atoms (T=Si or Al) with the amount of occluded K^+ and the total cation content much smaller than that required to balance the amount of Al generally encountered in merlinoite, which forces the Si/Al ratio of the zeolite to increase. Thus, it appears that encapsulation of the large TEA^+ cation within the zeolite pores is responsible for the observed increase in the Si/Al ratio, in agreement with other studies on different low-silica zeolites containing large organic cations.⁷

Thermogravimetric and differential thermal analyses of our merlinoite reported here in flowing air are in sharp contrast to those previously reported for other merlinoites (Fig. 3). At temperatures up to 270 °C there is a large weight loss associated with an endothermic process that we attribute to the desorption of occluded water. At temperatures above 350 °C there is a smaller weight loss in an exothermic process centred at around 500 °C, assigned to burning of the TEA^+ cations. The tempera-

†The expansion coefficient is defined as $\alpha = (V_x/V_0 - 1)/x$ where x is the molar fraction of Al and V_x and V_0 are the cell volumes for an Al fraction of x and 0, respectively. Here V_0 is obtained from the fitted linear correlation in Fig. 2.

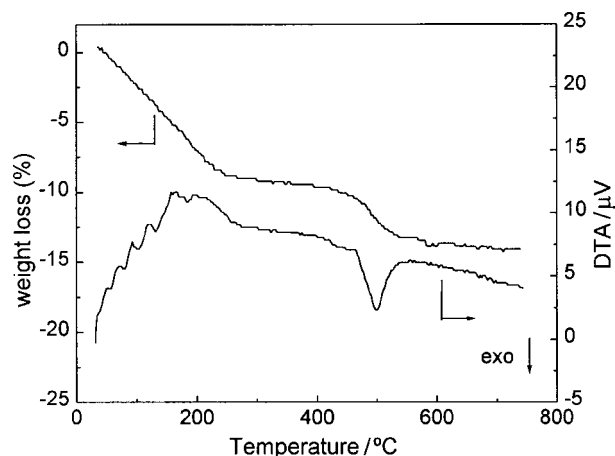


Fig. 3 Thermogravimetric and differential thermal traces of as-made merlinoite.

ture of the exothermic maximum is around 75 °C higher than that found for TEA^+ compensating for AlO_4^- species in the zeolite beta framework,¹⁴ probably reflecting diffusional problems within the smaller pores of merlinoite. Notably, the water content (*ca.* 12 $H_2O/u.c.$) is nearly half that observed in other natural and synthetic merlinoites (typically 20–24 $H_2O/u.c.$),^{5,11,15} probably due again to the increase in Si/Al ratio and to the large volume occupied by TEA^+ . More conclusively, calcined merlinoite loses 11.6% weight up to around 280 °C, which corresponds to around 15.5 H_2O molecules per unit cell, *i.e.* a 25–35% reduction in the water uptake that we must ascribe to a decreased hydrophilicity due to the enhanced Si/Al ratio.

The synthetic merlinoite reported here shows a very good thermal stability. Calcination at 580 °C removes the organic cation with only a marginal loss of crystallinity (>90% retained). Furthermore, *in situ* XRD experiments in static air show a relatively good stability of the structure of the calcined material even up to 900 °C, although upon further heating at 1000 °C significant structure collapse occurs (Fig. 4). This is in stark contrast to the reported stability of a synthetic merlinoite containing Na^+ , K^+ and Sr^{2+} cations, which began losing crystallinity at 350 °C.¹³ While the improved thermal stability can be in part attributed to the enhanced Si/Al ratio, we believe the cation content may also have a strong influence on the stability. Thus, after NH_4^+ exchange the stability is

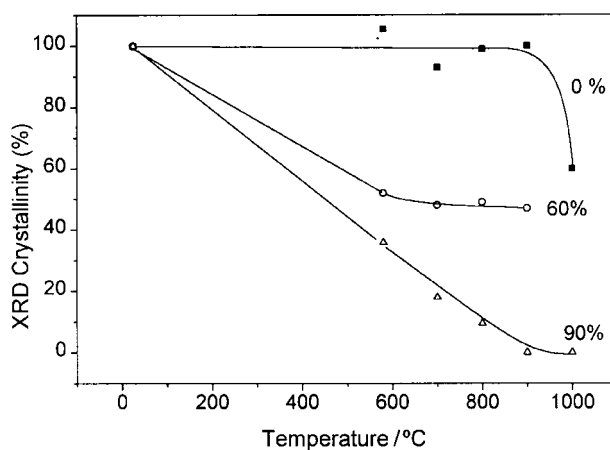


Fig. 4 Crystallinity of calcined merlinoite determined by XRD at different degrees of NH_4^+ exchange (indicated near each plot) as a function of the temperature during *in situ* thermal treatment under ambient air.

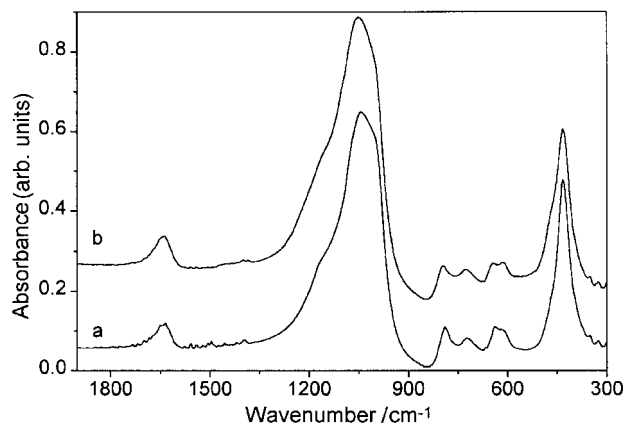


Fig. 5 IR spectra of as-made (a) and calcined (b) merlinoite in the framework vibrational region.

reduced inasmuch as K^+ is exchanged by NH_4^+ (Fig. 4). This seems to reflect a low stability of the acidic form of the zeolite.

The IR spectra of as-made and calcined merlinoite in the framework vibrational range (Fig. 5) are very similar to that reported by Belhekar *et al.* for merlinoite containing Na^+ , K^+ and Sr^{2+} cations,¹³ confirming the isomorphism of both materials. However, there are significant blue shifts in the spectrum of our material, in agreement with its enhanced Si/Al ratio. This is particularly clear for the most intense asymmetric stretching band which appears at 1046 cm^{-1} in our calcined sample and at around $1000\text{--}980\text{ cm}^{-1}$ in the spectrum given in ref. 13 (reported at 1006 cm^{-1} for zeolite W by Breck).¹⁶

SEM photographs show an unusual habit for the crystallites of merlinoite synthesised in this work (Fig. 6). Natural merlinoite typically appears as pseudo-tetragonal prismatic crystals elongated along the *c*-axis and terminated by orthorhombic prisms.¹⁰ Usually, synthetic merlinoite-type crystals have also an elongated prismatic shape.^{5,12,13} In contrast, most of the crystallites of the merlinoite presented here are not elongated but appear to be cuboids of $1 \times 1 \times 1$ to $3 \times 3 \times 3\ \mu\text{m}^3$. These cuboids show flat and clean faces together with rough faces. In the few crystallites which do actually show a small elongation, the rough faces are perpendicular to the direction of elongation.

^{29}Si MAS NMR of the as-made and calcined merlinoite are depicted in Fig. 7. Three well resolved resonances at $\delta -109$, -103 and -98 are clearly distinguished. There is also a low intensity shoulder at lower field ($\delta -93$). These lines are assigned to $\text{Si}[4\text{Si}, (4-n)\text{Al}]$ species with $n=0, 1, 2$ and 3 , respectively, and the one for $n=1$ is the most prominent one. The reported spectrum of a K^+ -containing merlinoite-type



Fig. 6 Scanning electron microscopy image of as-made merlinoite.

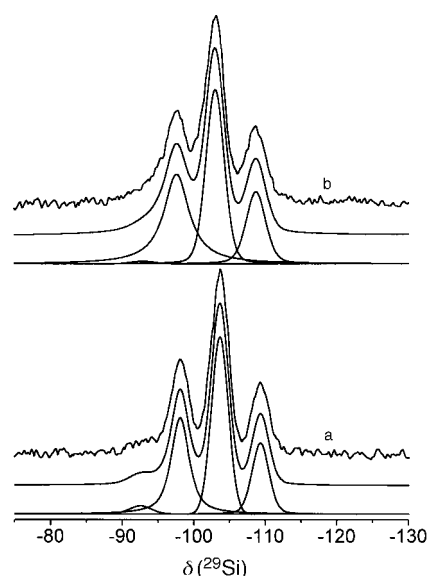


Fig. 7 ^{29}Si MAS NMR spectra of as-made (a) and calcined (b) merlinoite. For each material the upper trace is the experimental spectrum with the simulation and the deconvoluted components depicted in the middle and bottom traces, respectively.

material with $\text{Si}/\text{Al}=2.1$ clearly showed five lines implicitly assigned to $n=0, 1, 2, 3$ and 4 , with the $n=2$ resonance being the most intense. These differences between both spectra [number and relative intensities of the $\text{Si}(n\text{Al})$ resonances] reflect the enhanced Si/Al ratio of our material. Actually, deconvolution of the spectra in Fig. 7 allowed us to calculate a Si/Al ratio of around 3.3 for both the as-made and calcined merlinoite materials presented here. This value, while slightly smaller than that found by chemical analysis, again confirms the enhanced Si/Al ratio of the zeolite. We note here that the chemical shift of every $\text{Si}(n\text{Si})$ resonance in the spectra in Fig. 7 is in good agreement with the values reported by Belhekar *et al.*,¹³ while disagreeing with those in ref. 5 where 5–6 ppm low-field shifts are apparent for every resonance. A calculation of the expected chemical shifts using the average T–O–Si angles given in ref. 5 and in this work (see below) and using the equations of Thomas *et al.*¹⁷ [for $\text{Si}(0\text{Al})$] or Radeaglia and Engelhardt¹⁸ [for $\text{Si}(n\text{Al})$] shows there to be a very close agreement with our chemical shift values and suggests the spectrum in ref. 5 was misreferenced.

The ^{27}Al MAS NMR spectra of the as-made and calcined merlinoites show a prominent resonance at $\delta 58.3$ and 58.6 , respectively, assigned to tetrahedral Al in the framework (Fig. 8). No octahedral aluminium signals are detected, sug-

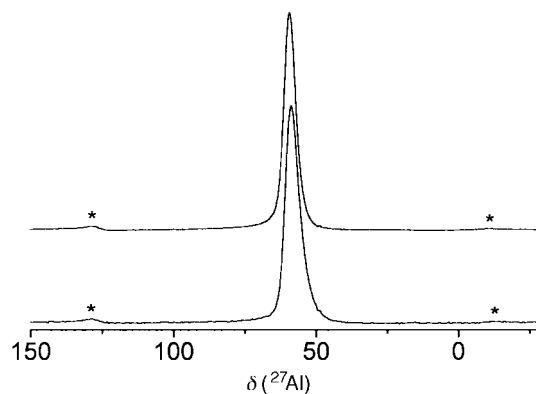


Fig. 8 ^{27}Al MAS NMR spectra of as-made (bottom) and calcined (top) merlinoite. Spinning side bands are marked with an asterisk.

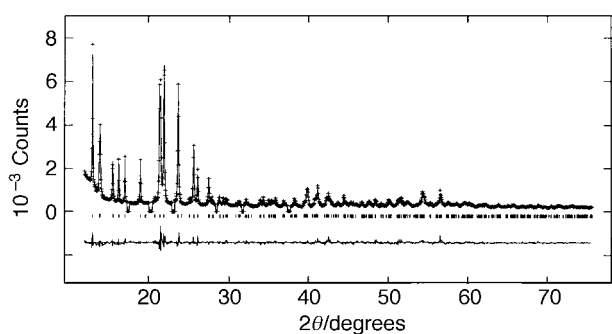


Fig. 9 Rietveld plot for merlinoite: experimental data (+), calculated (—) and difference (lower trace). Tick marks represent the positions of allowed reflections. Note the excluded regions represent a small quantity ($\approx 1\%$) of a zeolite beta impurity phase.

gesting there is little, if any, dealumination occurring during the calcination.

Structure

The true topological symmetry for the merlinoite framework (structure code MER)¹⁹ is tetragonal, space group $I4/mmm$.¹² However like Bieniok *et al.*⁵ we too observe that the refinement is better in the orthorhombic subgroup $Immm$, although no actual splitting of the peaks is observed in the diffraction pattern, with the deviation from the idealised tetragonal symmetry being much lower in our case ($a-b=0.0017 \text{ \AA}$ cf. 0.1078 \AA in ref. 5). This can be understood by the lower Al and K content in our material which is again reflected in the lower unit cell volume obtained here [$1982.06(22) \text{ \AA}^3$] with respect to the earlier reported materials (see Fig. 2 above). The final Rietveld plot in $Immm$ is given in Fig. 9 and the final atomic positions in Table 4. Selected distances and angles for framework and extraframework atoms are given in Tables 5 and 6, respectively. In $Immm$ two T-sites are present in the asymmetric unit both of which from the average T—O distances (1.637 and 1.656 \AA) are thought to contain the Al ions in this structure. The two principal potassium sites seen in the difference Fourier maps are observed to be close to the positions K(1) and K(2) found by Bieniok *et al.*⁵

Since the refined occupancy for these two sites was found to be close to that expected from chemical analysis the other sites found from analysis of the Fourier maps were assigned to water positions. We note however that one of the assigned water positions, OW(2), is close to one of the sites suggested in the earlier work to be a K position but refinement of this as a third K site led to a higher than expected potassium content per unit cell and a lower water content. It did prove

Table 4 Positions of framework atoms, isotropic temperature factors and occupancy for merlinoite (Si/Al=3.8) with esds in parentheses

Atom	<i>x</i>	<i>y</i>	<i>z</i>	$U_{\text{iso}}/\text{\AA}^2$	Occupancy
Si(1)	0.1093(5)	0.2686(6)	0.1534(7)	0.0329(19)	1.0
Si(2)	0.2585(6)	0.1135(5)	0.1588(6)	0.0339(20)	1.0
O(1)	0.1174(10)	0.3144(12)	0	0.016(5)	1.0
O(2)	0.2893(12)	0.1327(14)	0	0.103(8)	1.0
O(3)	0	0.2314(14)	0.1587(20)	0.046(4)	1.0
O(4)	0.2486(12)	0	0.2123(11)	0.023(6)	1.0
O(5)	0.1632(11)	0.1679(11)	0.1927(7)	0.056(7)	1.0
O(6)	0.1453(8)	0.3428(9)	0.2657(14)	0.036(4)	1.0
K(1)	0.1715(13)	0.5	0	0.177(9)	0.915(13)
K(2)	0	0.3398(13)	0	0.047(9)	0.467(15)
OW(1)	0.5	0.4646(25)	0.5	0.120(8)	0.426(17)
OW(2)	0.5	0.5	0.2473(15)	0.120(8)	0.800(18)
OW(3)	0	0.5	0.3310(25)	0.120(8)	0.919(15)
OW(4)	0	0.4746(26)	0	0.120(8)	0.5
OW(5)	0.4140(17)	0.3442(17)	0	0.120(8)	0.631(12)

Table 5 Framework bond distances (\AA) and angles ($^\circ$) with esds in parentheses

Si(1)—O(1)	1.659(10)	O(1)—Si(1)—O(3)	102.7(11)
Si(1)—O(3)	1.633(9)	O(1)—Si(1)—O(5)	121.3(7)
Si(1)—O(5)	1.659(10)	O(1)—Si(1)—O(6)	110.4(9)
Si(1)—O(6)	1.595(17)	O(3)—Si(1)—O(5)	98.6(8)
		O(3)—Si(1)—O(6)	119.4(9)
		O(5)—Si(1)—O(6)	104.9(6)
Si(2)—O(2)	1.658(10)	O(2)—Si(2)—O(4)	118.3(9)
Si(2)—O(4)	1.696(7)	O(2)—Si(2)—O(5)	110.2(8)
Si(2)—O(5)	1.587(18)	O(2)—Si(2)—O(6)	99.5(9)
Si(2)—O(6)	1.658(15)	O(4)—Si(2)—O(5)	108.8(7)
		O(4)—Si(2)—O(6)	105.7(7)
		O(5)—Si(2)—O(6)	114.2(6)
		Si(1)—O(1)—Si(1)	133.3(12)
		Si(2)—O(2)—Si(2)	143.9(14)
		Si(1)—O(3)—Si(1)	142.3(13)
		Si(2)—O(4)—Si(2)	142.1(8)
		Si(1)—O(5)—Si(2)	139.0(6)
		Si(1)—O(6)—Si(2)	144.4(8)

Table 6 Extraframework atom distances (\AA) with esds in parentheses

Pair	Distance (\AA)	Frequency per unit cell
K(1)—O(1)	2.731(18)	2
K(1)—O(4)	3.071(14)	2
K(1)—O(6)	3.449(16)	4
K(1)—OW(4)	2.449(20)	2
K(2)—O(2)	3.002(19)	2
K(2)—O(6)	3.122(16)	4
K(2)—OW(3)	2.818(22)	2
K(2)—OW(5)	2.870(32)	2

possible to refine a more idealised model for this structure whereby OW(2) was assigned to a K site and water molecules close to Wyckoff sites 2c and 2d [OW(1) and OW(4)] were constrained onto these positions since in the absence of this added condition the model is less stable. The refined potassium content of *ca.* 6.2 and total water content of *ca.* 15.3 molecules per unit cell are still close to that expected. However, it was noticeable that the framework bond distances and angles as well as the temperature factors for the extraframework sites were less satisfactory despite the fact that the agreement factors were comparable to the earlier model. For these reasons we have maintained our model with two K sites but can not rule out the possibility that there is some disorder over the sites occupied by the extraframework atoms.

The merlinoite topology comprises an interconnected set of 8MR channels of different dimensions, ([100] $3.1 \times 3.5 \text{ \AA}$, [010] $2.7 \times 3.6 \text{ \AA}$, [001] $3.4 \times 5.1 \text{ \AA} + 3.3 \times 3.3 \text{ \AA}$)¹⁹ and directed along each of the three principal crystallographic directions. Fig. 10 shows sections of the channel system along the [001] and [010] directions illustrating the positions of the extraframework sites. In Fig. 10(a), the K(1) sites (large circles) can be distinguished lying in the $3.3 \times 3.3 \text{ \AA}$ channel with their coordination made up by four framework oxygens and approximately two water molecules. The K(2) position is found at the centre of the channel parallel to [010] coordinating to four framework oxygens forming the eight ring window as well as to approximately four water molecules. The remaining extraframework sites treated here as water molecules are found within the $3.4 \times 5.1 \text{ \AA}$ channel lying parallel to [001]. We postulate that the template in the as-prepared material may well reside in the relatively large cage formed by the crossing of this channel and the ones running along [100] and [010]. Monte Carlo type solids docking calculations undertaken using the Biosym Insight II software²⁰ showed this to be a possible location for the template in this structure.

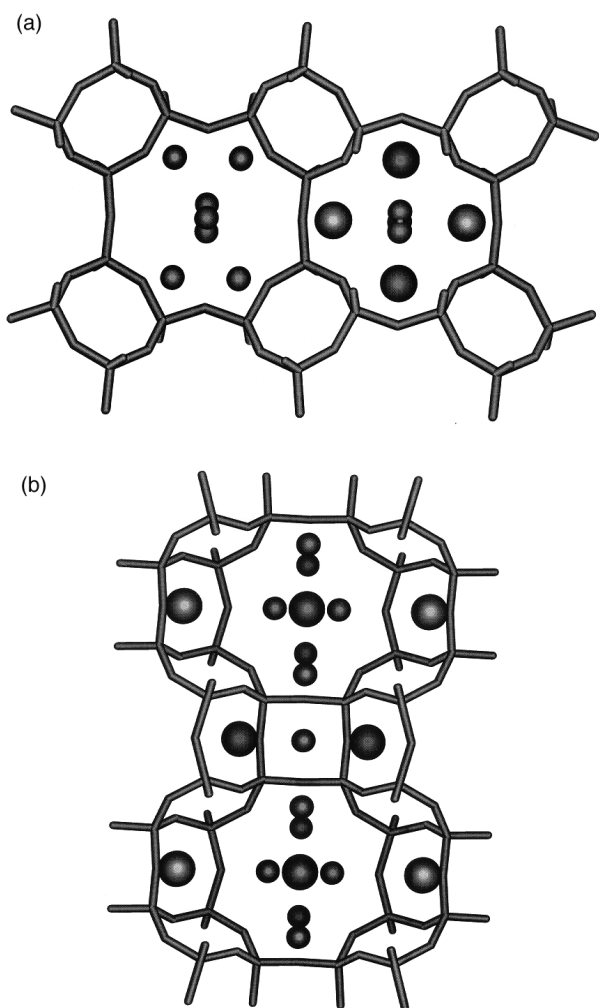


Fig. 10 Merlinoite framework viewed in the [001] (a) and [010] (b) directions. The zeolite framework is represented by sticks, potassium cations sites by large spheres and water positions by small spheres.

Conclusions

Merlinoite can be synthesised with a significantly enhanced Si/Al ratio by using tetraethylammonium during the synthesis. This large cation is occluded in the zeolite channels as a pore-filling agent and hence limits the concentration of cations,

thus lowering the amount of framework Al. The enhanced Si/Al ratio of the zeolite is reflected by a number of characteristics including blue shifts in the framework vibration bands, a lower unit cell volume, a decreased distortion from the tetragonal symmetry, a reduced hydrophilicity and an improved thermal stability.

The authors gratefully acknowledge financial support by the Spanish CICYT (project MAT97-0723). We thank the CLRC for provision of the synchrotron radiation facilities and Dr. C. Tang for assistance with the data collection. P.A.B. is grateful to the European Union TMR program for a postdoctoral fellowship.

References

- 1 R. Aiello and R. M. Barrer, *J. Chem. Soc., A*, 1970, 1470.
- 2 R. M. Barrer and P. J. Denny, *J. Chem. Soc.*, 1961, 971.
- 3 H. M. Rietveld, *J. Appl. Crystallogr.*, 1969, **2**, 65.
- 4 A. Larson and R. B. Von Dreele, GSAS Manual, Los Alamos Report No. LA-UR-86-746.
- 5 A. Bieniak, K. Bornholdt, U. Brendel and W. H. Baur, *J. Mater. Chem.*, 1996, **6**, 271.
- 6 J.B. Hastings, W. Thomlinson and D. E. Cox, *J. Appl. Crystallogr.*, 1984, **17**, 85.
- 7 R. M. Barrer, *Hydrothermal Chemistry of Zeolites*, Academic Press, London, 1982.
- 8 M. A. Cambor and J. Pérez-Pariente, *Zeolites*, 1991, **11**, 202.
- 9 M. A. Cambor, A. Corma, A. Mifsud, J. Pérez-Pariente and S. Valencia, *Stud. Surf. Sci. Catal.*, 1997, **105**, 341.
- 10 R. W. Tschernich, *Zeolites of the World*, Geoscience Press Inc., Phoenix, 1992.
- 11 R. J. Donahoe, B. C. Hemingway and J. G. Liou, *Am. Mineral.*, 1990, **75**, 188.
- 12 L. P. Solov'eva, S. V. Borisov and V. V. Bakakin, *Sov. Phys. Crystallogr.*, 1972, **16**, 1035.
- 13 A. A. Belhekar, A. J. Chandwadkar and S. G. Hedge, *Zeolites*, 1995, **15**, 535.
- 14 M. A. Cambor, A. Corma and S. Valencia, *Microporous and Mesoporous Materials*, in press.
- 15 E. Galli, G. Gottardi and D. Pongiluppi, *N. Jb. Miner. Mh.*, 1979, **H.1**, 1.
- 16 D. W. Breck, *Zeolite Molecular Sieves: Structure, Chemistry and Use*, John Wiley & Sons, New York, 1974.
- 17 J. M. Thomas, J. Klinowski, S. Ramdas, B. K. Hunter and D. T. B. Tennakoon, *Chem. Phys. Lett.*, 1983, **102**, 158.
- 18 R. Radeglia and G. Engelhardt, *Chem. Phys. Lett.*, 1985, **114**, 28.
- 19 W. M. Meier, D. H. Olson and Ch. Baerlocher, *Atlas of Zeolite Structure Types*, Elsevier, London, 4th edn., 1996.
- 20 Insight II, Biosym Technologies Inc., 9265 Scranton Road, San Francisco, 1994.

Paper 8/03801E